Published in final edited form as:
Clin Cancer Res. 2008 December 1; 14(23): 7682–7690. doi:10.1158/1078-0432.CCR-08-1328.

Constitutive Activation of STAT5 Contributes to Tumor Growth, Epithelial-Mesenchymal Transition, and Resistance to EGFR Targeting

Priya Koppikar[1,*], **Vivian Wai Yan Lui**[2,*], **David Man**[1], **Sichuan Xi**[1], **Raymond Liu Chai**[1], **Elizabeth Nelson**[1], **Allison BJ Tobey**[1], and **Jennifer Rubin Grandis**[1,3]

[1]Department of Otolaryngology, University of Pittsburgh, Pittsburgh, PA 15213, USA

[2]Department of Clinical Oncology, Room 302, Sir YK Pao Centre for Cancer, Prince of Wales Hospital, The Chinese University of Hong Kong, Shatin, Hong Kong

[3]Department of Pharmacology, University of Pittsburgh, Pittsburgh, PA 15213, USA

Abstract

Purpose—Signal Transducer and Activator of Transcription 5 (STAT5) is activated in squamous cell carcinoma of the head and neck (SCCHN), where targeting STAT5 inhibits tumor growth *in vitro* and *in vivo*. The role of STAT5 activation in carcinogenesis, tumor progression and response to therapy remains incompletely understood. In this study, we investigated the effects of STAT5 activation in squamous epithelial carcinogenesis and respond to therapy.

Experimental Design—The functional consequences of STAT5 activation in squamous epithelial carcinogenesis were examined using cells derived from normal (Het-1A) and transformed mucosal epithelial cells engineered to express constitutive-active mutants of STAT5.

Results—The growth rate of stable clones derived from both normal and transformed squamous epithelial cells expressing the constitutive-active STAT5 were increased. In SCCHN xenografts, tumor volumes were increased in constitutive-active STAT5 mutant cells compared to vector-transfected controls. Constitutive activation of STAT5 significantly increased cell migration and invasion through Matrigel as well as the transforming efficiency of SCCHN cells *in vitro* as assessed by soft agar assays. The constitutive-active STAT5 clones derived from SCCHN cells demonstrated changes consistent with an epithelial-mesenchymal transition (EMT) including decreased expression of E-cadherin and increased vimentin, in comparison to control transfectants. In these cells, STAT5 activation was associated with resistance to cisplatin-mediated apoptosis and growth inhibition induced by the EGFR tyrosine kinase inhibitor (TKI), erlotinib.

Conclusions—These results suggest that constitutive STAT5 signaling enhances tumor growth, invasion and EMT in squamous epithelial carcinogenesis and may contribute to resistance to EGFR TKI and chemotherapy.

Keywords

STAT5; SCCHN; EMT; EGFR; tyrosine kinase inhibitor

Corresponding Author: Jennifer Rubin, Grandis Corresponding Address: Suite 500 Eye and Ear Institute, 203 Lothrop Street, University of Pittsburgh, Pittsburgh, PA 15213, Telephone number: 412-647-5280, Fax number: 412-383-5409, jgrandis@pitt.edu.
*Both authors contributed equally to this work

Introduction

Signal Transducer and Activator of Transcription 5 (STAT5), a transcription factor that is activated by tyrosine phosphorylation, regulates gene expression when stimulated by a wide variety of growth factors, hormones and cytokines (1). Activated STAT5 dimers bind to specific DNA response elements in the promoter region of target genes in the nucleus and regulate various cellular responses, including growth, migration, survival and cell motility. Two highly homologous forms of STAT5, STAT5a and STAT5b, are encoded by two closely linked genes on human chromosome 17q11.2. Cumulative evidence suggests that STAT5 isoforms may display distinct as well as redundant functions.

STAT5 activation has been implicated in oncogenesis. Studies in hematopoietic malignancies suggest that STAT5 may be necessary and sufficient for malignant transformation (2). Emerging evidence also supports an important role for STAT5 in solid tumors. STAT5 is constitutively activated in several solid tumors including prostate cancer (3, 4), breast cancer (5), nasopharyngeal carcinoma (6) and squamous cell carcinoma of the head and neck (SCCHN) (7). However, the precise role of STAT5 in epithelial carcinogenesis remains incompletely understood.

The functional consequences of STAT5 activation appear to depend on the cellular context. In prostate cancer, constitutive activation of STAT5 correlated with high histological grade and early disease recurrence (3, 4). In contrast, activated STAT5 correlated with increased patient survival in breast cancer and nasopharyngeal cancer, indicating that STAT5 maybe a favorable prognostic factor in these malignancies (5, 6).

We previously reported constitutive activation of STAT5 downstream of EGFR in SCCHN compared with normal oral epithelial cells from unaffected individuals where STAT5 activation was higher in the SCCHN tumors compared to levels in the corresponding normal mucosa from the same SCCHN patients (7). Further investigation demonstrated that specific targeting of STAT5 isoforms by antisense oligonucleotides resulted in abrogation of STAT5 expression and activation, inhibition of SCCHN growth *in vitro* and *in vivo,* as well as inhibition of expression of STAT5 target genes (7, 8). Thus, loss of function studies have implicated a role for STAT5 activation in SCCHN proliferation.

The present study was undertaken to test the hypothesis that constitutive activation of STAT5 contributes to SCCHN tumorigenesis and response to therapy. EGFR is emerging as a therapeutic target in several cancers including SCCHN. Despite promising results in preclinical models, the response rate to tyrosine kinase inhibitors (TKI) or monoclonal antibodies as monotherapy is no greater than 10–13% in the setting of recurrent or metastatic disease (8–10). We studied the functional consequences of constitutive STAT5 activation in two representative SCCHN cell lines and in non-transformed immortalized squamous epithelial cells, using stable expression of constitutive-active mutants of STAT5. Our results suggest that constitutive STAT5 signaling enhances tumor growth, invasion and EMT in squamous epithelial carcinogenesis, as well as contributes to the resistance of SCCHN cells to apoptosis and growth inhibition induced by cisplatin or the EGFR TKI erlotinib, respectively.

Materials and Methods

Reagents

Antibodies used include E-cadherin (BD Biosciences Pharmingen, San Diego, CA), Vimentin (Sigma-Aldrich, St.Louis, MO), p-Tyr PY99 (Santa Cruz Biotechnology, Inc, Santa Cruz, CA), anti-STAT5a rabbit antiserum and anti-STAT5b rabbit antiserum (Santa

Cruz Biotechnology, Inc, CA), GAPDH (Abcam Inc, Cambridge, MA) and Beta-actin (Calbiochem, San Diego, CA). The ECL kit was from Santa Cruz Biotechnology, Inc (Santa Cruz, CA). Geneticin (G418) was from Invitrogen (Carlsbad, CA). The EGFR specific tyrosine kinase inhibitor, erlotinib (Tarceva®) was obtained from Genentech (South San Francisco, CA).

Plasmids

The vector control plasmid, pUSEamp(+), was purchased from Upstate Biotechnology (Charlottesville, VA). Plasmids carrying the activated mutant of STAT5a and STAT5b (pMX STAT5a 1*6 and pMX STAT5b 1*6 plasmids, respectively) [kind gifts from Dr. Toshio Kitamura (University of Tokyo, Japan) (36)] were subcloned into the pUSEamp(+) backbone. Briefly, the STAT5 activated mutant genes were released from the pMX STAT5a 1*6 or pMX STAT5b 1*6 plasmids by restriction digestion with EcoRI and SalI, which was then cloned into the EcoRI and XhoI sites of the pUSEamp (+) vector. The subcloned plasmids, which carried a CMV promoter, were named as pUSTAT5a 1*6 and pUSTAT5b 1*6, respectively. The sequence of the plasmids was confirmed by automated sequencing (University of Pittsburgh, Pittsburgh, PA). The beta-casein luciferase reporter gene, beta-casein Luc, and the E-cadherin Luc constructs were kind gifts from Dr. Richard Jove (H. Lee Moffitt Cancer Center & Research Institute, Orlando, FL) and Dr. J. Torchia at the University of Wisconsin, respectively.

Cell culture and generation of stable clones

SCCHN cell lines PCI-15B and UM-22B are of human origin (12). A human esophageal cell line, Het-1A, was purchased from ATCC (Manassas, VA). SCCHN cells were maintained in DMEM with 10 % fetal calf serum (Mediatech, Herndon, VA). Het-1A cells were maintained in Airway epithelial cell culture medium with supplements (PromoCell, Heidelberg, Germany) and 2 % fetal calf serum (Invitrogen, Carlsbad, CA) with 1x Penicillin/Streptomycin (Gibco, Carlsbad, CA). Cell lines were cultured at 37°C with 5 % CO_2 in humidified incubators. For stable clone generation, cells were transfected with pUSTAT5a 1*6 and pUSTAT5b 1*6 plasmids with Lipofectamine 2000 (Invitrogen, Carlsbad, CA). Two days after transfection, transfectants were maintained in G418 selection medium. Single colonies were isolated and maintained in G418 selection medium (0.8 mg/ml for PCI-15B clones; 2 mg/ml for UM-22B and 0.4 mg/ml for Het-1A clones).

Luciferase assays

Stable clones were screened for increase in STAT5 transcriptional activity using beta-casein luciferase reporter gene. Transient transfection of stable clones (3×10^5 cells) was performed using 2 μg of beta-casein luciferase plasmid in 6 well plates. Five hours after transfection, the medium was replaced with complete medium. 24–48 hrs post transfection, cells were lysed in luciferase lysis buffer (0.05% Triton X-100, 2 mM EDTA and 0.1 M Tris-HCl at pH 7.8) for 5 mins on ice. Lysates were then centrifuged at 14, 000 rpm for 5 min at 4°C. Supernatants were collected and assayed for luciferase activity using the luciferase assay kit from Promega (Madison, WI). Luminescence was measured with a luminometer (Wallac Inc., Gaithersburg, MD). Luciferase activity was expressed as relative light units per microgram of total protein (RLU/μg protein). Fold changes in transcriptional activity with reference to the respective vector transfected control cells were calculated.

Western blotting

Cells were lysed with the western lysis buffer (1 % Nonidet-P40, 150 mM NaCl, 1 mM EDTA, 10 mM sodium phosphate buffer (pH 7.2), 0.25 mM DTT, 1 mM PMSF, 10 g/ml leupeptin and 10 g/ml aprotinin) for 5 mins at 4°C The lysate was then centrifuged at 4°C,

12000 rpm for 10 mins. Supernatant was collected for protein quantitation. Protein quantitation was performed using the Protein Assay Solution (BioRad Laboratories, Hercules, CA) and bovine serum albumin of known concentration as the standard. Fifty μg of total protein was resolved on 8 % SDS-PAGE gel and transferred onto the Trans-Blot nitrocellulose membrane (BioRad Laboratories, Hercules, CA) using the semi-dry transfer machine (BioRad Laboratories, Hercules, CA). Membranes were probed for specific antibodies as previously described (7).

In vitro growth

Equal number of cells were plated in 12-well dishes and allowed to adhere overnight. Cell proliferation was followed every day up to 4 days. Cells were harvested by trypsinization and cell numbers, in triplicates, were determined by counting (with the trypan blue dye) using a hemocytometer.

Soft agar colony formation assay

Briefly, 0.2×10^5 cells were plated in triplicate in a 0.35% agarose layer (with low-melting agarose) on top of a 0.7 % prechilled agarose layer in a 60 mm tissue culture dish. Both layers contained 1x complete medium. After plating, the tissue culture dishes were chilled at 4°C to solidify the agarose before they were incubated at 37°C (and 5% CO_2) for 2–4 weeks. Colonies were then stained with p-iodonitrotetrazolium violet solution in 1x PBS (1 mg/ml) (Sigma, St. Louis, MO). Number of colonies in 9 random fields was counted under a light microscope at 40X magnification.

Matrigel invasion assay

Cellular invasion was quantified with BD Biocoat Matrigel Invasion Chambers with 8 M pore size (BD Biosciences, Bedford, MA, USA) according to the manufacturer's instructions. Briefly, the filter inserts and lower chambers were rehydrated with 250 and 500 microliters complete medium respectively, and incubated at 37°C for two hours. 4×10^4 cells in complete media were then seeded onto the Matrigel-coated fibers and incubated for 24 hours. Post-incubation, the non-invading cells were removed from the upper surface of the filter insert with cotton-tipped swabs and then stained with Protocol Hema 3 Manual Staining System (Fisher Scientific, Swedesboro, NJ, USA). Invading cells were counted under 200X magnification from 4 randomly selected fields per samples and mean values from several independent assays performed in duplicate were calculated.

Cell migration assay

At 90–95% confluence, the cells were quiesced in medium without serum for 36–48 hours. A wound was induced with a sterile tip, after which the cells were treated with complete medium and incubated at 37°C for 24 hours. Photographs were taken at 0 (immediately after wound induction) and 24 hours, and relative distance traveled by the cells at the acellular front was determined by computer assisted image analysis.

Tumor xenograft studies

Four- to six-week old female athymic nude mice (nu/nu; Harlan Sprague Dawley, Indianapolis, IN) (n=5) were subcutaneously injected with 1×10^6 PCI-15B STAT5a 1*6 #2 cells on the right flank and 1×10^6 PCI-15B pUSEamp #1 cells on the left flank. Tumors were measured with calipers every 5 days after inoculation and tumor volumes were calculated with the formula: volume= length × $\text{width}^2/2$. Animal care was in strict compliance with institutional guidelines established by the University of Pittsburgh, the Guide for the Care and Use of Laboratory Animals [National Academy of Sciences (1996)],

and the Association for Assessment and Accreditation of Laboratory Animal Care International.

In vitro apoptosis assay

0.4×10^5 cells of PCI-15B pUSEamp #1 and PCI-15B STAT5a 1*6 #2 were plated in complete DMEM, with or without 10 μM cisplatin, which was added after the cells were allowed to adhere overnight. 24 hrs post drug treatment, cells were detached by trypsinization, counted and pelleted (1000 rpm for 5 min) Cell pellets were washed once with PBS (pH 7.4) and resuspended in 100 μl of Annexin V binding buffer (10mM HEPES, pH 7.4; 140 mM NaCl; 2.5 mM $CaCl_2$). 5 μl of Annexin V-Cy3 (BioVision Research Products, Mountain View, CA) was added per tube and allowed to incubate at room temperature for 15 min in the dark. Then, the stained cell suspension was dropped on clean slides and covered with coverslips. The membrane of apoptotic cells stained a bright orange color when analyzed by fluorescence microscopy. The ratio (percentage) of apoptotic to total cells (apoptotic plus non apoptotic) was calculated for each high power field. For each treatment, 5–10 high power fields of view were quantitated on each section.

Erlotinib treatment of STAT5 dominant active and vector control transfected cells

0.2×10^5 of PCI-15B pUSEamp #1 and PCI-15B STAT5a 1*6 #2 cells were plated in complete medium in 12-well plates. Twenty-four hours later, cells were treated with erlotinib (10 μM). Cell counts were performed 48 hours after treatment, using trypan blue vital dye exclusion. Precent inhibition of cell growth induced by erlotinib was calculated compared with DMSO treated controls for both PCI-15B pUSEamp #1 and PCI-15B STAT5a 1*6 #2 cells. Each treatment was carried out in triplicate, and the experiment was repeated six times.

Statistics

The StatXact software with Cytel Studio (Cytel Software Corporation, Cambridge, MA, USA) was used for statistical analysis. Comparisons of *in vitro* cell proliferation, transforming efficiency, cellular migration and invasion; apoptosis and erlotinib-mediated growth inhibition were performed using the exact one-tailed (Wilcox-Mann-Whitney) test. *In vivo* tumor growth experiments compared the tumor volume in one flank to the paired tumor volume in the opposite flank with the one-tailed sign ranked test, under the *a priori* assumption that tumors derived from the STAT5 constitutive-active cells would be higher in volume when compared to those derived from the vector-transfected cells.

Results

Generation of SCCHN and immortalized squamous epithelial cells expressing dominant-active STAT5

We previously reported that STAT5 was activated in SCCHN downstream of EGFR and Src family kinases (7, 8, 11). To elucidate the role of STAT5 activation in head and neck carcinogenesis, we established stable clones expressing constitutive-active mutants of STAT5 in two representative SCCHN cell lines (PCI-15B and UM-22B) and an immortalized mucosal squamous epithelial cell line (Het-1A). The constitutive-active mutants were generated by PCR-driven random mutagenesis under a retroviral promoter leading to either of 2 mutations that results in constitutive tyrosine phosphorylation of STAT5 isoforms (both STAT5a and STAT5b) in the absence of growth factor stimulation (12) (Figure 1A). The mutant STAT5 plasmids were subcloned under a CMV promoter to replace the retroviral promoter of the parent construct and cells were transfected with the vector alone (pUSEamp), or plasmids expressing constitutive-active mutants of STAT5.

Upon long-term G418 selection, stable clones expressing the activated mutants were isolated and screened by beta-casein luciferase reporter assays. Consistent with prior reports, stable expression of either STAT5a 1*6 or STAT5b 1*6 in these cell lines resulted in tyrosine phosphorylation of both STAT5a and STAT5b in co-immunoprecipitation assays (12) (13), thereby limiting our ability to examine the consequences of activation of the individual STAT5 isoforms (data not shown). Transcriptional activity in the STAT5 stably transfected clones was evaluated by luciferase assays (Figure 1B,C,D). The PCI-15B stable clones STAT5a 1*6 #2 and STAT5b 1*6 #15 showed a 10-fold and 4.1-fold increase in transcriptional activity compared to the pUSEamp #1 control clone, indicating these clones expressed the constitutive active STAT5 mutants. Similarly, the UM-22B STAT5a 1*6 #4 clone showed a 12-fold increase in transcriptional activity compared to the vector control UM-22B pUSEamp #1. The Het-1A STAT5a 1*6 #6 clone showed a 9.5-fold increase in transcriptional activity when compared to the vector-transfected control Het-1A pUSEamp #3.

Activation of STAT5 increases SCCHN and normal epithelial cell proliferation *in vitro* and SCCHN growth *in vivo*

In order to examine the biological consequence of STAT5 activation on cell growth in both SCCHN and non-transformed mucosal epithelial cells, the growth rates of SCCHN and Het-1A stably transfected with the STAT5a constitutive-active mutants were evaluated. As shown in Figure 2, the growth rates of PCI-15B STAT5a 1*6 #2, PCI-15B STAT5b 1*6#15 and Het-1A STAT5a 1*6 #6 were higher than that of the respective vector-transfected control cells (Figures 2A and 2B) (p=0.004).

Since STAT5 activation resulted in enhanced proliferation *in vitro*, we next examined if STAT5 activation would affect the growth of SCCHN tumors *in vivo*. A two-flank xenograft model was used to assess growth of stably transfected SCCHN cells in nude mice. Growth rates of the SCCHN xenografts were followed for up to 25 days after inoculation. PCI-15B STAT5a 1*6 #2 and PCI-15B STAT5b 1*6 #15 derived tumors grew significantly faster (p=0.03125) than those derived from the control clone (PCI-15B pUSEamp #1) (Figure 2C). However, inoculation of Het-1A STAT5a 1*6 #6 cells in nude mice did not lead to tumor formation (data not shown) suggesting that while STAT5 activation may contribute to SCCHN growth *in vivo*, STAT5 activation alone is not be sufficient to transform normal squamous epithelial cells.

STAT5 activation results in increased transforming efficiency in SCCHN

STAT5 can potentiate the transforming activity of other oncogenes, such as v-Src (11), as well as function as a transforming oncogene in hematopoietic cells (2). To determine whether STAT5 activation can contribute to cancer initiation in SCCHN, we examined the effect of STAT5 activation on the transforming efficiency of SCCHN cells using a soft agar colony formation assay. As shown in Figure 3, the PCI-15B STAT5a 1*6 #2 and PCI-15B STAT5b 1*6 #15 clones, but not the Het-1A STAT5a 1*6 #6 clone (data not shown), showed a significant increase in the number of transforming colonies when compared with the respective vector-transfected control (PCI-15B STAT5a 1*6 #2: 51.78 2.56 colonies, PCI-15B STAT5b 1*6 #15: 48.00 2.38 colonies versus PCI-15B pUSEamp #1: 16.8 1.3 colonies; n=9 fields, p<0.0001).

STAT5 activation increases SCCHN migration and invasion

STAT5 has been implicated in cell migration and/or invasion in prostate cancer and kidney epithelial cells (4, 14). To determine if STAT5 activation was associated with normal and/or transformed mucosal epithelial cell migration, Het-1A pUSEamp #3, Het-1A STAT5a 1*6 #6, PCI-15B pUSE amp #1 and PCI-15B STAT 5a 1*6 #2 cells were seeded onto 12-well

plates and grown until 90–95% confluent, followed by serum starvation for 36–48 hours, after which a wound was induced and cell migration was measured at 24 hours post wound induction. Het-1A constitutive-active STAT5 cells (Het-1A STAT 5a 1*6 #6) were only modestly more motile than the vector-transfected control cells (data not shown). However, in SCCHN cells, we observed a mean 8.5-fold increase in migration (equivalent to fold decrease in area of wound) compared to the vector-transfected control cells ($p=0.05$; Figure 4A). To determine the functional consequence of STAT5 activation on the invasive potential of SCCHN we examined the invasion of SCCHN cells expressing constitutive-active STAT5 through Matrigel. Stable clones expressing the vector-transfected control (PCI-15B pUSEamp #1) showed no detectable invasion (0.00 cells/well ± 0.00 SEM) while the PCI-15B STAT5a 1*6 #2 and STAT5b 1*6 #15 clones were invasive (13.70 cells/well ± 4.356 SEM; $p<0.001$, and 17.10 cells/well ± 4.557 SEM; $p<0.001$, respectively) (Figure 4B). The vector-transfected control Het-1A clone was minimally invasive and its capacity to invade was not significantly increased by expression of constitutive-active STAT5 (data not shown). These results demonstrate that activation of STAT5 increases the migration and invasive potential of SCCHN cells, but is not sufficient to induce migration and/or invasion of non-transformed squamous epithelial cells.

Activation of STAT5 abrogates E-cadherin and increases vimentin expression in SCCHN

Reduced expression of E-cadherin is associated with an increased risk of tumor invasion and metastasis in several cancers (15–17). Loss of E-cadherin and increase in vimentin expression is consistent with an epithelial to mesenchymal transition (EMT), a central process implicated in cancer invasion and metastasis (17). Since we observed an increase in cellular migration through Matrigel, we next examined if these alterations induced by STAT5 activation were consistent with EMT. Expression of E-cadherin in PCI-15B STAT5 activated cells (PCI-15B STAT5a 1*6 #2 and PCI-15B STAT5b 1*6 #15) was lost and vimentin expression was elevated when compared to expression levels in the vector-transfected control cells (PCI-15B pUSEamp #1) (Figure 5A). Consistent with the induction of EMT markers, PCI-15B STAT5a 1*6 #2 cells showed distinct morphological alterations when compared with vector-transfected control cells (PCI-15B pUSEamp #1) (Figure 5B). The latter demonstrated a more pleomorphic and attached morphology compared with the SCCHN cells expressing activated STAT5, which showed a cell scattering phenotype that was less adherent. To further investigate the reduction of E-cadherin expression levels in STAT5 dominant active clones, we performed luciferase assays in PCI-15B cells co-transfected transiently with either E-cadherin Luc and pUSE amp(+) constructs or E-cadherin Luc and pUSTAT5a 1*6 constructs. 48 hours after transfection, cells were lysed and luciferase assays were performed. As shown in Figure 5C, co-transfection of E-cadherin Luc and pUSTAT5a 1*6 caused reduction in transcriptional activity of E-cadherin Luc by more than 50% ($p=0.002$). This suggests that dominant active STAT5 causes transcriptional repression of E-cadherin. However, this transcriptional repression may not be the only mechanism for the complete loss of E-cadherin expression as seen in Figure 5A, and other factors such as promoter methylation or mutation in the E-cadherin gene may be involved. Transcriptional repression of E-cadherin by STAT5b has been demonstrated before (18).

Activation of STAT5 increases resistance to cisplatin-induced apoptosis and erlotinib-induced growth inhibition

STAT5 activation has been associated with resistance to apoptotic stimuli (19, 20) although in other models, expression of constitutive-active STAT5 resulted in apoptosis of IL-3 independent BaF/3 cells, upon IL-3 treatment (21). We previously demonstrated that chemotherapeutic agents including cisplastin induced SCCHN cell death through apoptosis (Xi et al, Oncogene 2005, Thomas SM et al, Mol Pharm 2008 D-please endnote). To determine the effects of STAT5 activation on apoptosis in SCCHN cell lines, we measured

the percentage of apoptotic cells upon addition of cisplatin (10 μM), a commonly used chemotherapeutic reagent in SCCHN. Cisplatin treatment of PCI-15B pUSEamp #1 cells resulted in significantly more apoptosis compared to the response in cells expressing constitutive-active STAT5 [36.825% (± 2.727% SEM) in PCI-15B pUSEamp #1 versus 6.4125% (± 1.1575% SEM) in PCI-15B STAT5a 1*6 #2]; (p=0.0143; Figure 6A). Similar responses were obtained using viability MTT assays where the cells expressing dominant-active STAT5 were more resistant to cisplatin than vector-transfected control cells(data not shown).

The EMT phenotype is associated with decreased *in vitro* sensitivity to the EGFR TKI, erlotinib in lung cancer (22, 23). Since constitutive activation of STAT5 induced markers associated with EMT, we next examined if activated STAT5 led to resistance to erlotinib. The IC_{50} value of erlotinib in PCI-15B pUSEamp#1 cells was determined to be 10 μM, which is consistent with most SCCHN cell lines examined (data not shown). PCI-15B cells express very high levels of EGFR where EGFR phosphorylation is inhibited by treatment with erlotinib (24). We detected significantly less growth inhibition induced by erlotinib treatment of the SCCHN cells expressing constitutive-active STAT5 (PCI-15B STAT5a 1*6 #2) compared with vector-transfected control cells (PCI-15B pUSE amp #1); (p=0.0011; Figure 6B), suggesting that STAT5 activation may contribute to the modest clinical responses observed when SCCHN patients receive EGFR TKIs.

Discussion

The role of STAT5 activation in cancer depends on the specific tumor type under investigation. We demonstrate here that STAT5 activation enhances the growth of normal and transformed squamous epithelial cells, increases migration and invasion of squamous carcinoma cells, and induces phenotypic and molecular changes associated with EMT. Our results are consistent with the reported oncogenic functions of STAT5 in a variety of hematopoietic malignancies and support a role for STAT5 activation in solid tumors. The translational significance is demonstrated by our finding that STAT5 activation is associated with resistance to cisplatin or erlotinib in SCCHN cells expressing dominant-active STAT5 isoforms.

STAT5 has been implicated as an oncogene, primarily in hematopoietic malignancies. The same constitutively activated STAT5a mutant that was used in the present study (S711F) was able to transform hematopoietic cell lines (2). In chronic myelogenous leukemia (CML), STAT5 activation has been shown to mediate the transforming activity of Bcr-Abl (25). Activation of STAT5a in myeloma and lymphoma associated with the TEL/JAK2 oncogenic gene fusion is independent of cell stimulus and has been shown to be essential for the tumorigenicity of the TEL/JAK2 oncogene (26). Indeed, activation of STAT5 is both necessary and sufficient for transformation by TEL/JAK2, and STAT5 activation, leading to induction of the single downstream target gene oncostatin M (OSM) and induction of a lethal myeloproliferative disease. STAT5 activation has been linked to transformation mediated by other fusion genes including NPM/ALK and TEL/ABL (27, 28). The STAT5b/retinoic acid receptor alpha gene fusion has been detected in a small subset of acute promyelocytic-like leukemias (APLL) (29).

Fewer studies have elucidated the role of STAT5 activation in solid tumors. In prostate cancers, STAT5 activation is a poor prognostic factor, where cumulative evidence implicates STAT5 in disease progression and recurrence (3, 4). In contrast, STAT5 activation is correlated with improved survival in breast and nasopharyngeal cancers (5, 6). We previously reported that STAT5 is activated in SCCHN, downstream of EGFR and/or Src family of kinases (7, 11). Using loss-of-function approaches, including antisense

oligonucleotides and dominant-negative mutants targeting STAT5 isoforms, we found that inhibition of STAT5b, but not STAT5a, abrogated SCCHN growth (7, 8). In the present study, we used a gain-of-function approach to introduce constitutive-active mutants of STAT5 into SCCHN and normal mucosal squamous epithelial cells. Forced overexpression of activating mutations of STAT5 is a more direct way to study the functional consequences and contribution of STAT5 activation. These double mutations are known to result in gain-of-function of STAT5 as reflected by constitutive tyrosine phosphorylation and enhanced transcriptional activity of STAT5 (12). While it is possible that activation of STAT5a may induce a phenotype that is inconsistent with our previous studies abrogating STAT5a (7), the persistent activation of STAT5b in the cells transfected with either dominant-active construct is the most likely explanation for the transforming potential of the STAT5a construct in the present study.

Constitutive activation of STAT5 resulted in increased cell proliferation of both normal and transformed squamous epithelial cells. STAT5, in concert with Raf, has been shown to induce proliferation in IL-3 dependant cell lines, abrogating the need for the addition of exogenous cytokines (12). Activated STAT5 also plays a role in cellular proliferation of a diverse phenotype of cells including primary endothelial cells (30), myeloid cells (31) as well as head and neck cancers (7).

Constitutively active mutants of STAT5 have been shown to be oncogenic *in vivo* and *in vitro* and are capable of restoring the defective functions of STAT5 null mice (2). In contrast to the profound effects of STAT5 activation on transformed squamous cells, activation of STAT5 in immortalized normal epithelial cells failed to enhance migration, invasion, or induce transformation. These findings suggest that unlike hematopoietic cells where STAT5 activation alone can lead to malignant transformation (2), other events are required in mucosal epithelial cells.

In addition to enhancing cell and tumor growth, increased STAT5 activation also increased SCCHN invasion. The role of STAT5 in tumor invasion and/or metastasis is incompletely understood. Our previous finding that STAT5 mediates erythropoietin-induced invasion in SCCHN suggests that STAT5 activation may be involved in tumor invasion (32). Here, we demonstrate that cell migration and invasion are, at least in part, a consequence of STAT5 activation in SCCHN.

Epithelial-to-mesenchymal transition (EMT) is a crucial embryogenic and developmental process during which epithelial cells acquire mesenchymal, fibroblast-like properties and show reduced intercellular adhesion and increased motility. Accumulating evidence points to a critical role of EMT-like events during tumor progression and malignant transformation, endowing the incipient cancer cell with invasive and metastatic properties (33). We found that activation of STAT5 resulted in phenotypic and molecular changes consistent with induction of EMT in transformed squamous epithelial cells. Further, STAT5 activation seems, at least partially, to cause transcriptional repression of E-cadherin (Figure 5C). Previous studies have shown that STAT5 may facilitate mesenchymal transition in kidney epithelial cells as well as enhance aggressive behavior of hepatocellular carcinomas via induction of EMT (18, 34). However, in breast cancer cells, dominant-negative STAT5 mutants resulted in the induction of invasion and EMT (35), implicating an invasion-suppressive role for STAT5 in breast cancer. Prolactin-induced STAT5 activation resulted in an invasion-suppressive phenotype, including an increase in E-cadherin expression and reduced invasion through Matrigel (35). The basis for the distinct roles of STAT5 in mediating invasion and EMT in different types of tumors are not entirely clear. Potential contributing factors include different cell types, tumor microenvironments and regulating upstream cytokines and growth factors.

Recently, EMT has been reported to serve as a determinant of sensitivity to EGFR inhibition by erlotinib in lung cancer (21, 22). Since constitutive STAT5 activation resulted in an EMT phenotype in SCCHN cells in our studies, we compared the sensitivity of constitutive-active STAT5 expressing SCCHN cells and vector-transfected control cells to the growth inhibiting effects of the EGFR tyrosine kinase inhibitor, erlotinib. We found that constitutive-active STAT5 expressing cells were less susceptible to growth suppression or apoptosis induced by erlotinib or cisplatin, respectively, in comparison to vector-transfected controls. These findings may have important implications for EGFR tyrosine kinase inhibitor therapy. Increased STAT5 activation and/or the transition to a mesenchymal type may provide a “molecular signature” to identify patients who are less likely to benefit from EGFR tyrosine kinase therapy.

Acknowledgments

This study was supported by NIH grant RO1CA77308-01 (to JRG).

Abbreviations

STAT	Signal transducer and Activator of Transcription
SCCHN	Squamous cell carcinoma of the head and neck
EMT	Epithelial-Mesenchymal Transition
EGFR	Epidermal growth factor receptor

References

1. Lin JX, Leonard WJ. The role of Stat5a and Stat5b in signaling by IL-2 family cytokines. Oncogene. 2000; 19:2566–76. [PubMed: 10851055]
2. Moriggl R, Sexl V, Kenner L, et al. Stat5 tetramer formation is associated with leukemogenesis. Cancer Cell. 2005; 7:87–99. [PubMed: 15652752]
3. Li H, Ahonen TJ, Alanen K, et al. Activation of signal transducer and activator of transcription 5 in human prostate cancer is associated with high histological grade. Cancer Res. 2004; 64:4774–82. [PubMed: 15256446]
4. Li H, Zhang Y, Glass A, et al. Activation of signal transducer and activator of transcription-5 in prostate cancer predicts early recurrence. Clin Cancer Res. 2005; 11:5863–8. [PubMed: 16115927]
5. Nevalainen MT, Xie J, Torhorst J, et al. Signal transducer and activator of transcription-5 activation and breast cancer prognosis. J Clin Oncol. 2004; 22:2053–60. [PubMed: 15169792]
6. Hsiao JR, Jin YT, Tsai ST, et al. Constitutive activation of STAT3 and STAT5 is present in the majority of nasopharyngeal carcinoma and correlates with better prognosis. Br J Cancer. 2003; 89:344–9. [PubMed: 12865928]
7. Xi S, Zhang Q, Gooding WE, Smithgall TE, Grandis JR. Constitutive activation of Stat5b contributes to carcinogenesis in vivo. Cancer Res. 2003; 63:6763–71. [PubMed: 14583472]
8. Leong PL, Xi S, Drenning SD, et al. Differential function of STAT5 isoforms in head and neck cancer growth control. Oncogene. 2002; 21:2846–53. [PubMed: 11973644]
9. Cohen EE, Rosen F, Stadler WM, et al. Phase II trial of ZD1839 in recurrent or metastatic squamous cell carcinoma of the head and neck. J Clin Oncol. 2003; 21:1980–7. [PubMed: 12743152]
10. Soulieres D, Senzer NN, Vokes EE, et al. Multicenter phase II study of erlotinib, an oral epidermal growth factor receptor tyrosine kinase inhibitor, in patients with recurrent or metastatic squamous cell cancer of the head and neck. J Clin Oncol. 2004; 22:77–85. [PubMed: 14701768]
11. Xi S, Zhang Q, Dyer KF, et al. Src kinases mediate STAT growth pathways in squamous cell carcinoma of the head and neck. J Biol Chem. 2003; 278:31574–83. [PubMed: 12771142]

12. Onishi M, Nosaka T, Misawa K, et al. Identification and characterization of a constitutively active STAT5 mutant that promotes cell proliferation. Mol Cell Biol. 1998; 18:3871–9. [PubMed: 9632771]

13. Lin CJ, Grandis JR, Carey TE, et al. Head and Neck Squamous Cell Carcinoma Cell Lines: Established Models and Rationale for Selection. Head and Neck. 2007 Published online in advance of print.

14. Benitah SA, Valeron PF, Rui H, Lacal JC. STAT5a activation mediates the epithelial to mesenchymal transition induced by oncogenic RhoA. Mol Biol Cell. 2003; 14:40–53. [PubMed: 12529425]

15. Tanaka M, Kitajima Y, Edakuni G, Sato S, Miyazaki K. Abnormal expression of E-cadherin and beta-catenin may be a molecular marker of submucosal invasion and lymph node metastasis in early gastric cancer. Br J Surg. 2002; 89:236–44. [PubMed: 11856141]

16. Yoshida R, Kimura N, Harada Y, Ohuchi N. The loss of E-cadherin, alpha- and beta-catenin expression is associated with metastasis and poor prognosis in invasive breast cancer. Int J Oncol. 2001; 18:513–20. [PubMed: 11179480]

17. Thiery JP. Epithelial-mesenchymal transitions in development and pathologies. Curr Opin Cell Biol. 2003; 15:740–6. [PubMed: 14644200]

18. Lee TK, Man K, Poon RT, et al. Signal transducers and activators of transcription 5b activation enhances hepatocellular carcinoma aggressiveness through induction of epithelial-mesenchymal transition. Cancer Res. 2006; 66:9948–56. [PubMed: 17047057]

19. Humphreys RC, Hennighausen L. Signal transducer and activator of transcription 5a influences mammary epithelial cell survival and tumorigenesis. Cell Growth Differ. 1999; 10:685–94. [PubMed: 10547072]

20. Shi M, Cooper JC, Yu CL. A constitutively active Lck kinase promotes cell proliferation and resistance to apoptosis through signal transducer and activator of transcription 5b activation. Mol Cancer Res. 2006; 4:39–45. [PubMed: 16446405]

21. Nosaka T, Kawashima T, Misawa K, et al. STAT5 as a molecular regulator of proliferation, differentiation and apoptosis in hematopoietic cells. Embo J. 1999; 18:4754–65. [PubMed: 10469654]

22. Thomson S, Buck E, Petti F, et al. Epithelial to mesenchymal transition is a determinant of sensitivity of non-small-cell lung carcinoma cell lines and xenografts to epidermal growth factor receptor inhibition. Cancer Res. 2005; 65:9455–62. [PubMed: 16230409]

23. Yauch RL, Januario T, Eberhard DA, et al. Epithelial versus mesenchymal phenotype determines in vitro sensitivity and predicts clinical activity of erlotinib in lung cancer patients. Clin Cancer Res. 2005; 11:8686–98. [PubMed: 16361555]

24. Boehm A, Sen M, Seethala RR, et al. Combined targeting of EGFR, STAT3, and Bcl-XL enhances antitumor effects in squamous cell carcinoma of the head and neck. Molecular Pharmacology. 2008 In Press.

25. Carlesso N, Frank DA, Griffin JD. Tyrosyl phosphorylation and DNA binding activity of signal transducers and activators of transcription (STAT) proteins in hematopoietic cell lines transformed by Bcr/Abl. J Exp Med. 1996; 183:811–20. [PubMed: 8642285]

26. Schwaller J, Parganas E, Wang D, et al. Stat5 is essential for the myelo- and lymphoproliferative disease induced by TEL/JAK2 [In Process Citation]. Mol Cell. 2000; 6:693–704. [PubMed: 11030348]

27. Nieborowska-Skorska M, Slupianek A, Xue L, et al. Role of signal transducer and activator of transcription 5 in nucleophosmin/anaplastic lymphoma kinase-mediated malignant transformation of lymphoid cells. Cancer Res. 2001; 61:6517–23. [PubMed: 11522649]

28. Spiekermann K, Pau M, Schwab R, et al. Constitutive activation of STAT3 and STAT5 is induced by leukemic fusion proteins with protein tyrosine kinase activity and is sufficient for transformation of hematopoietic precursor cells. Exp Hematol. 2002; 30:262–71. [PubMed: 11882364]

29. Arnould C, Philippe C, Bourdon V, et al. The signal transducer and activator of transcription STAT5b gene is a new partner of retinoic acid receptor alpha in acute promyelocytic-like leukaemia. Hum Mol Genet. 1999; 8:1741–9. [PubMed: 10441338]

30. Gomez D, Reich NC. Stimulation of primary human endothelial cell proliferation by IFN. J Immunol. 2003; 170:5373–81. [PubMed: 12759411]

31. Ilaria RL Jr, Hawley RG, Van Etten RA. Dominant negative mutants implicate STAT5 in myeloid cell proliferation and neutrophil differentiation. Blood. 1999; 93:4154–66. [PubMed: 10361113]

32. Lai SY, Childs EE, Xi S, et al. Erythropoietin-mediated activation of JAK-STAT signaling contributes to cellular invasion in head and neck squamous cell carcinoma. Oncogene. 2005; 24:4442–9. [PubMed: 15856028]

33. Larue L, Bellacosa A. Epithelial-mesenchymal transition in development and cancer: role of phosphatidylinositol 3′ kinase/AKT pathways. Oncogene. 2005; 24:7443–54. [PubMed: 16288291]

34. Kazansky AV, Rosen JM. Signal transducers and activators of transcription 5B potentiates v-Src-mediated transformation of NIH-3T3 cells. Cell Growth Differ. 2001; 12:1–7. [PubMed: 11205741]

35. Sultan AS, Xie J, LeBaron MJ, et al. Stat5 promotes homotypic adhesion and inhibits invasive characteristics of human breast cancer cells. Oncogene. 2005; 24:746–60. [PubMed: 15592524]

36. Trigo J, Hitt R, Koralewski P, et al. Cetuximab monotherapy is active in patients (pts) with platinum-refractory recurrent/metastatic squamous cell carcinoma of the head and neck (SCCHN): Results of a phase II study. American Society of Clinical Oncology. 2004; 2004:Abstract No 5502.

Statement of Clinical Relevance

Activation of Signal Transducer and Activator of Transcription (STAT)5 has been reported in a variety of malignancies where blockade of STAT5 inhibits cancer growth in preclinical cancer models. Generation of dominant-active mutants of STAT5 led to the observation that STAT5 activation was sufficient to transform hematopoietic cells. In these studies, we demonstrate that expression of dominant-active STAT5 mutants increases the growth and invasion of SCCHN cells in vitro and in vivo, but is not sufficient to transform normal mucosal epithelial cells. Further investigation demonstrated that increased STAT5 activation conferred an epithelial-to-mesenchymal (EMT) phenotype as well as resistance to cisplatin chemotherapy and EGFR inhibition. We previously reported that STAT5 is activated downstream of EGFR in squamous cell carcinoma of the head and neck (SCCHN). EGFR targeted therapy was FDA-approved for SCCHN 2006. However, despite the ubiquitous expression of EGFR in SCCHN tumors, only a subset of patients will respond to EGFR targeting. The translational implications of the present study suggest that STAT5 activation may contribute to therapeutic resistance in SCCHN where strategies that specifically inhibit STAT5 may improve therapeutic responses.

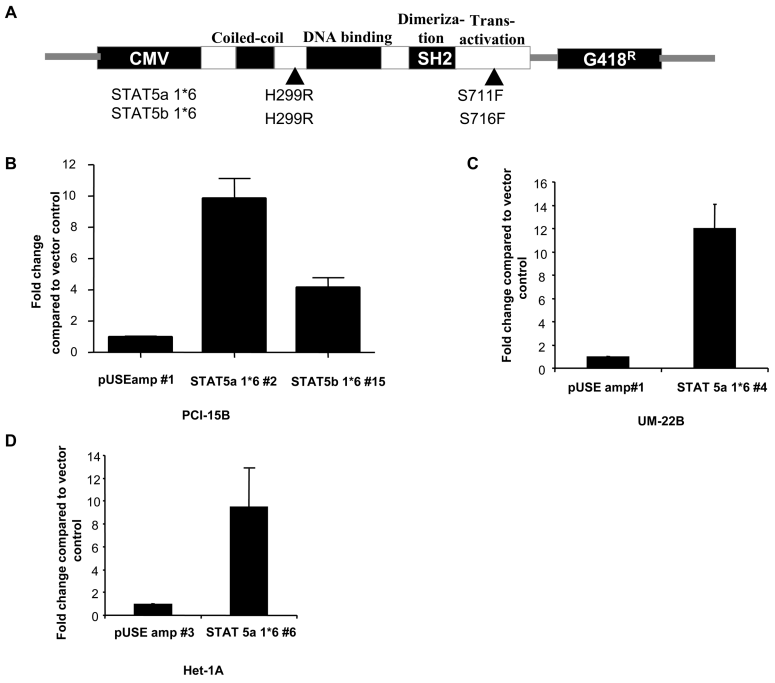

Figure 1. Increased STAT5 promoter activity and target gene expression is detected in cells transfected with dominant-active STAT5 isoforms

Stable clones using DA STAT5 isoforms were generated (A) by transfection with pUSEamp (+) (vector control), pUSTAT5a 1*6 (activated STAT5a) and pUSTAT5b 1*6 (activated STAT5b) plasmids in SCCHN cells (B) PCI-15B and (C) UM-22B and (D) Het-1A cells. Upon G418 selection, stable clones were isolated from the SCCHN cell lines and the immortalized mucosal epithelial cell line and screened for increase in STAT5 transcriptional activity using a beta-casein luciferase reporter gene construct. Luciferase activity was expressed as relative light units per microgram of total protein (RLU/g protein). Fold-change compared to the respective vector transfected cells were calculated. Experiments were performed 3 times with similar results.

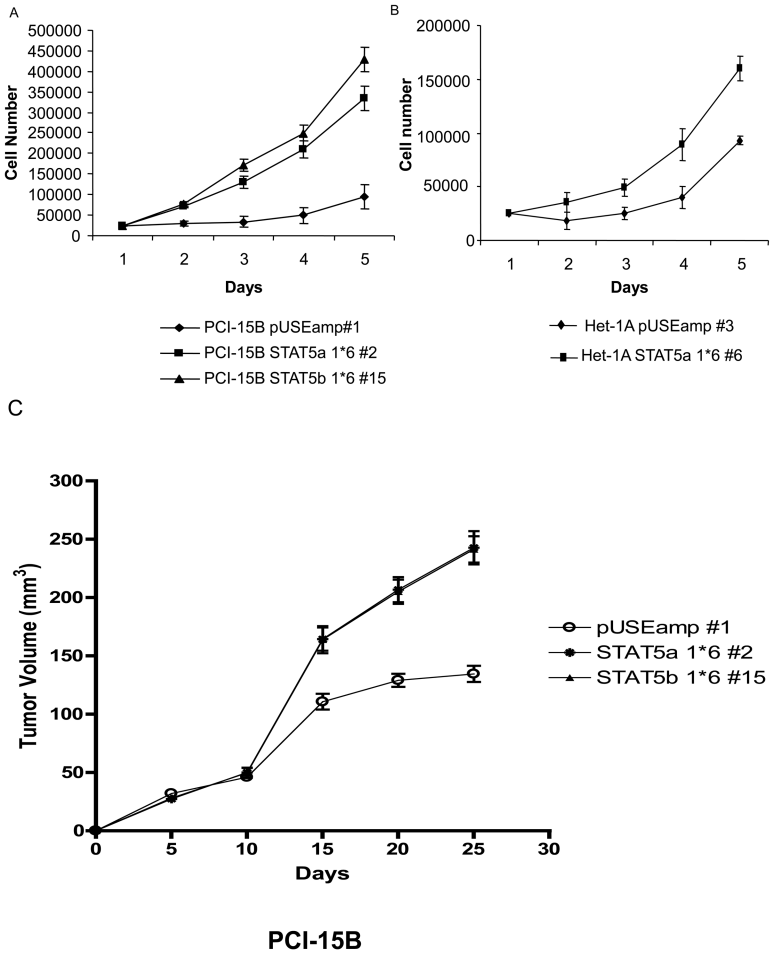

Figure 2. Activation of STAT5 induces SCCHN and normal epithelial cell proliferation *in vitro*

Representative STAT5 constitutive-active stable clones in the cell lines, (A) PCI-15B, and (B) Het-1A, were plated in triplicate at equal densities in complete growth medium. The growth rates of the STAT5 constitutive-active clones (PCI-15B STAT5a 1*6 #2 and Het-1A STAT5a 1*6 #6) were compared to growth rates of their respective vector-control transfected cells (PCI-15B pUSE amp#1 and Het-1A pUSE amp#3), cell growth was determined by cell counting. Viable cells were counted using trypan blue exclusion dye. The number of vector-transfected control cells and STAT5 constitutive-active cells were compared at day 2 after plating. PCI-15B STAT5a grew 1.496 fold faster than the vector control PCI-15B pUSE amp #1 (n=5 experiments, p=0.004), while Het-1A STAT5a 1*6 #6 grew 1.56 fold faster than its vector control Het-1A pUSE amp #3 (n=3 experiments, p=0.05). (C) Activation of STAT5 induces SCCHN growth *in vivo*. One million PCI-15B STAT5a 1*6 #2 cells were inoculated on the right flank of the nude mice (n=5) and one million PCI-15B pUSEamp #1 cells on the left flank (n=5). Tumor volumes were measured every 5 days after inoculation for up to 25 days. At day 15, tumor derived from PCI-15B STAT5a1*6 #2 clone grew significantly faster than that from the control clone, PCI-15B pUSEamp #1 (p=0.03125). At day 25, the tumor volume of PCI-15B STAT5a 1*6 #2 clone were 80.35 % greater than that of the control PCI-15B pUSEamp #1 clone (p=0.03125).

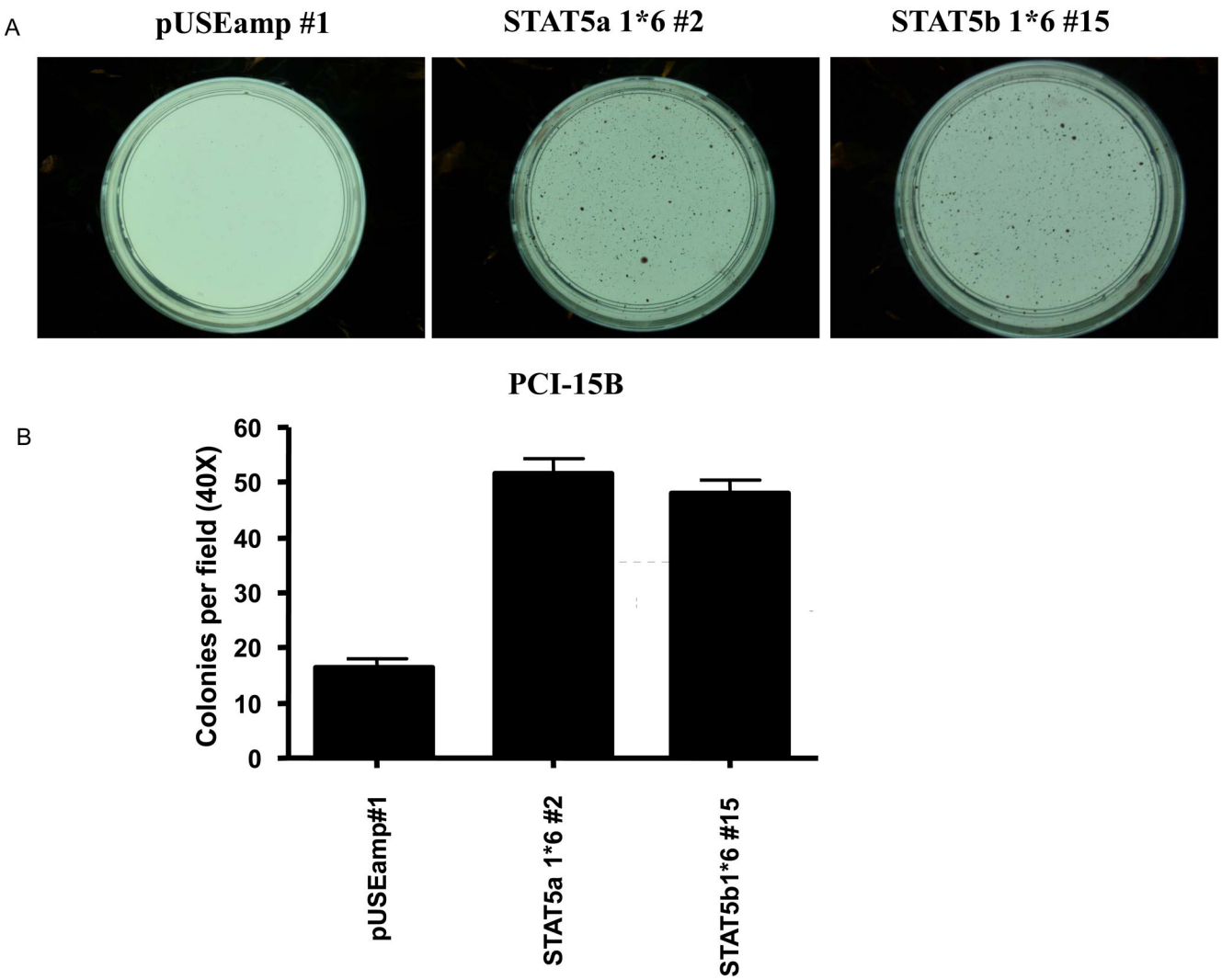

Figure 3. STAT5 activation results in increased growth of SCCHN cells in soft agar

Stable clones of PCI-15B pUSEamp #1 and PCI-15B STAT5a 1*6 #2 were plated in triplicate at a density of 0.2×10^5 cells/plate in soft agar containing 1x complete DMEM medium. Two-four weeks after plating, colonies were stained with p-iodonitrotetrazolium violet. (A) Representative stained colonies of PCI-15B pUSEamp #1, PCI-15B STAT5a 1*6 #2 and PCI-15B STAT5b 1*6 #15 are shown at 4X magnification. (B) The number of colonies in nine random fields was counted under a light microscope at 40X magnification. The bar graph represents mean ± SEM value, $p<0.0001$.

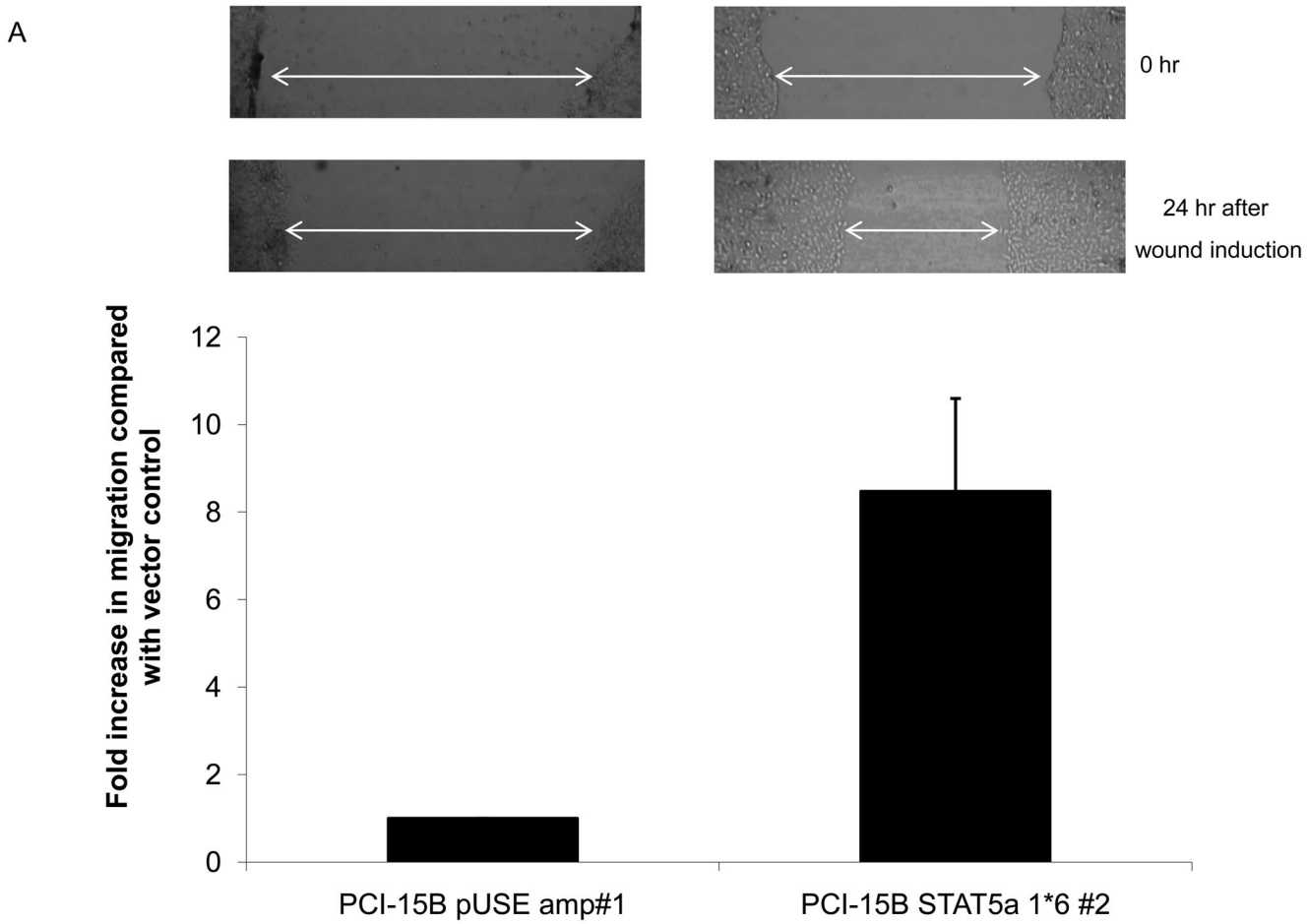

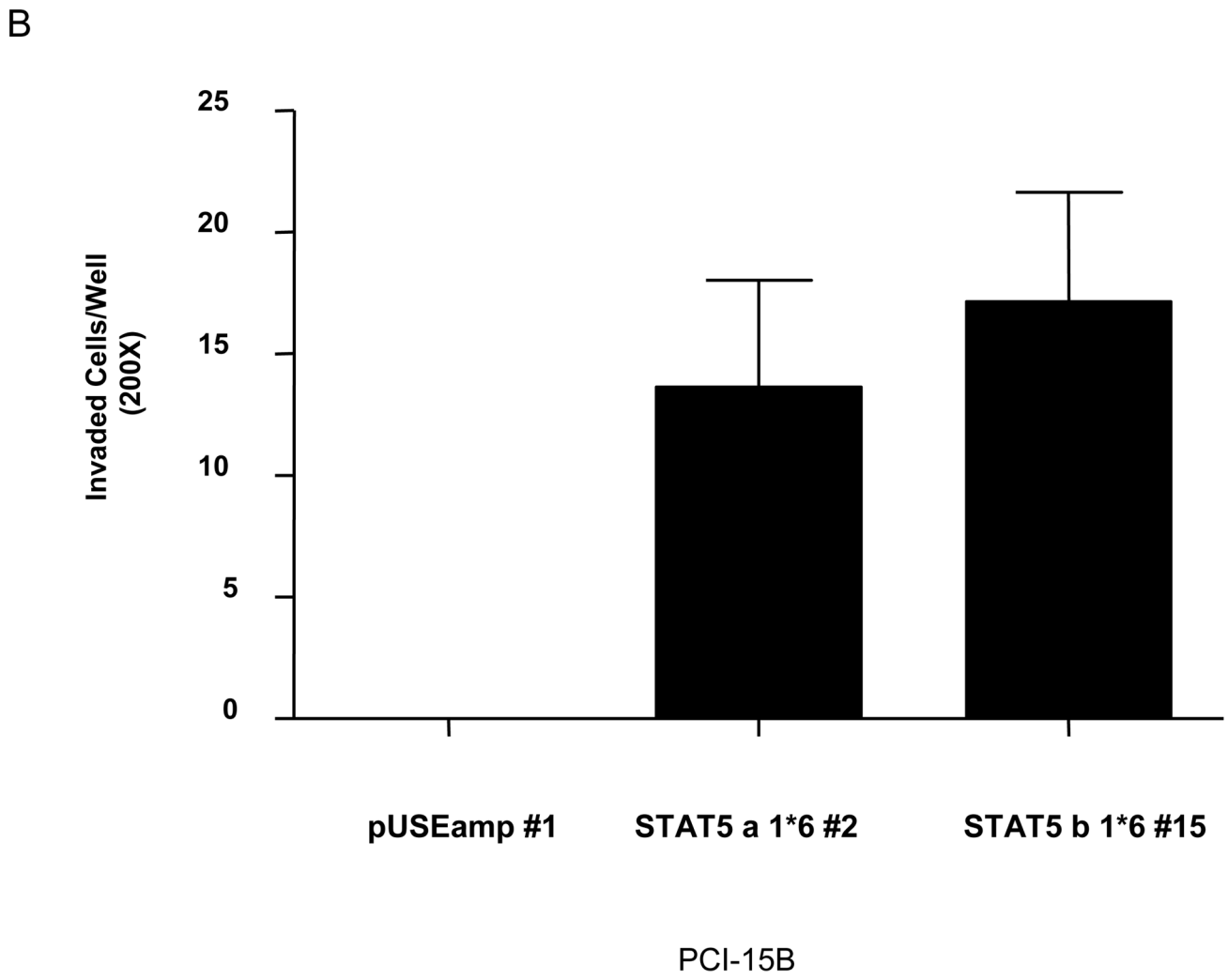

Figure 4. STAT5 activation increases SCCHN, but not normal epithelial cell migration and invasion

(A) SCCHN cells (PCI-15B pUSEamp #1 and PCI-15B STAT5a 1*6 #2) were grown until 90–95% confluent in 12-well plates and then serum starved for 36 hours. A wound was induced with a sterile tip and cell migration was monitored after 24 hours. Photographs were taken immediately after wound induction and 24 hours later (upper panel), and the relative distance traveled by the cells at the acellular front was determined by computer assisted image analysis (indicated by the arrow bars in the photographs). Cellular migration was determined by the decrease in total area of the wound after 24 hours. The graph indicates fold increase in migration of PCI-15B STAT 5a 1*6 #2 compared with the vector-transfected cells, PCI-15B pUSE amp #1, and represents cumulative data from 3 independent experiments ($p=0.05$). (B) PCI-15B stable clones were plated (4×10^4 cells) in complete medium onto Matrigel. Both the upper and the lower chambers were filled with complete medium. Twenty-four hours post-incubation, non-invading cells were removed from the upper surface of the filter insert and only invading cells were stained and counted (at 200X magnification) from randomly selected fields (n=4). The bar graph represents the mean ± SEM value for the SCCHN cells from several independent experiments that were performed in duplicate ($p=0.004$).

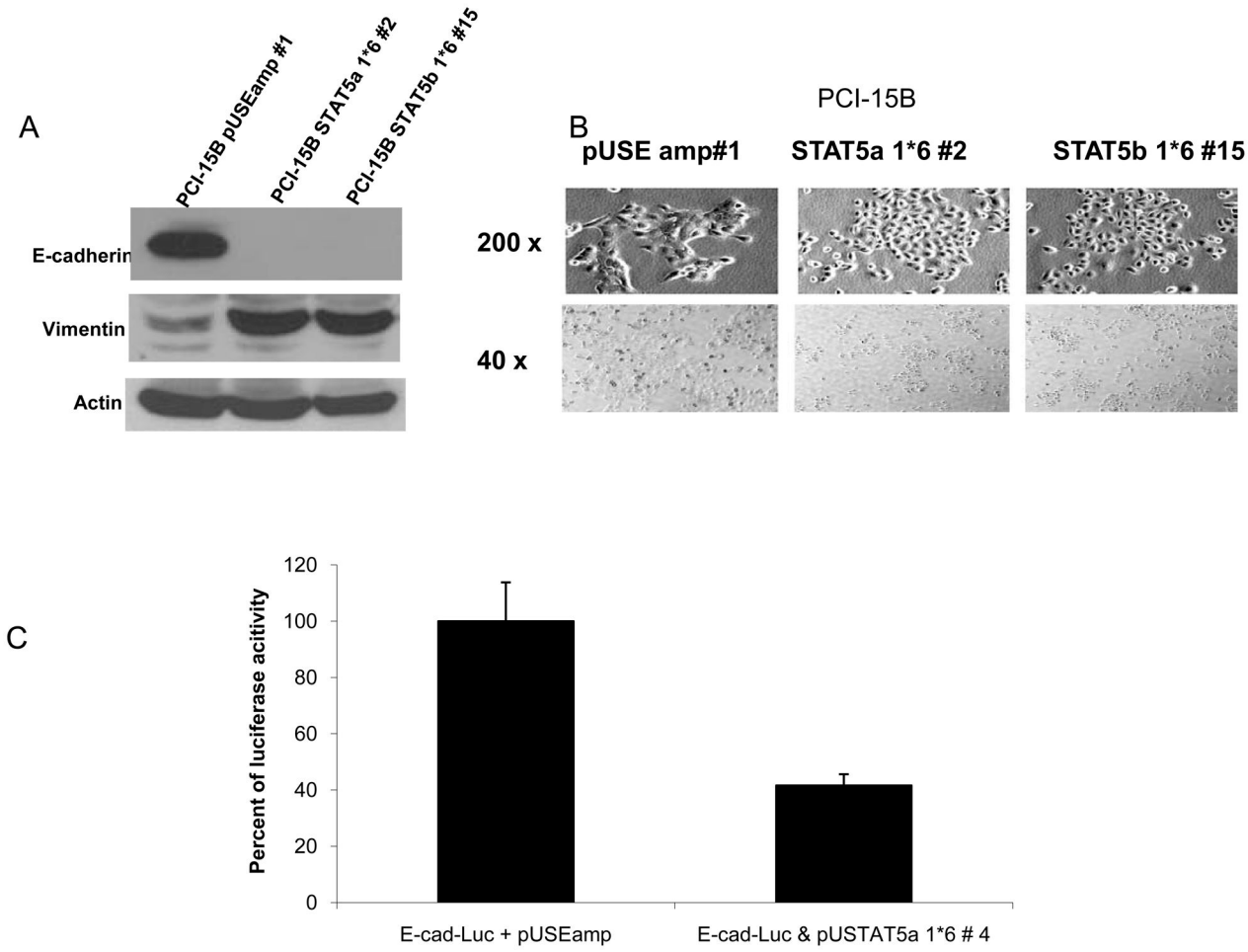

Figure 5. Activation of STAT5 induces molecular and phenotypic changes consistent with EMT

(A) Activation of STAT5 abrogates E-cadherin expression and increases vimentin expression in SCCHN cells. PCI-15B pUSEamp #1 cells and cells from two representative STAT5 dominant-active clones; PCI-15B STAT5a 1*6 #2 and PCI-15B STAT5b 1*6 #15, were harvested for Western blot analysis. Expression of E-cadherin was totally abrogated in the STAT5 constitutive-active cells when compared with the PCI-15B pUSEamp #1 control. The loss of E-cadherin was accompanied by an increase in vimentin expression. Actin is shown as loading control. (B) Activation of STAT5 results in cell scattering and reduced cell-cell adhesion in SCCHN cells. The stable clones, PCI-15B pUSEamp #1 and PCI-15B STAT5a 1*6 #2 were plated (3×10^5 cells, each) in tissue culture dishes. Twenty-four hours after plating, cellular morphology was recorded by digital camera under a microscope (at 40X and 200X magnification). The experiment was performed twice with similar results. (C) 3×10^5 cells of of PCI-15B cells were plated in triplicates in 6 well plates. 24 hours after plating, cells were transiently co-transfected with either 1.5 μg of E-cadherin Luc and 1.5 μg of pUSE amp (+) or 1.5 μg of E-cadherin Luc and 1.5 μg of pSTAT5a DA plasmids. Luciferase assay was performed 48 hours after transfection. Luciferase activity was expressed as relative light units per microgram of total protein (RLU/g protein). RLU/μg values from vector control and E-cadherin-Luc transfected cells were normalized to 100%, and decrease in RLU/μg of pSTAT5a DA and E-cadherin Luc transfected cells was calculated (p=0.002). P values were calculated from several independent experiments, performed in triplicate each time.

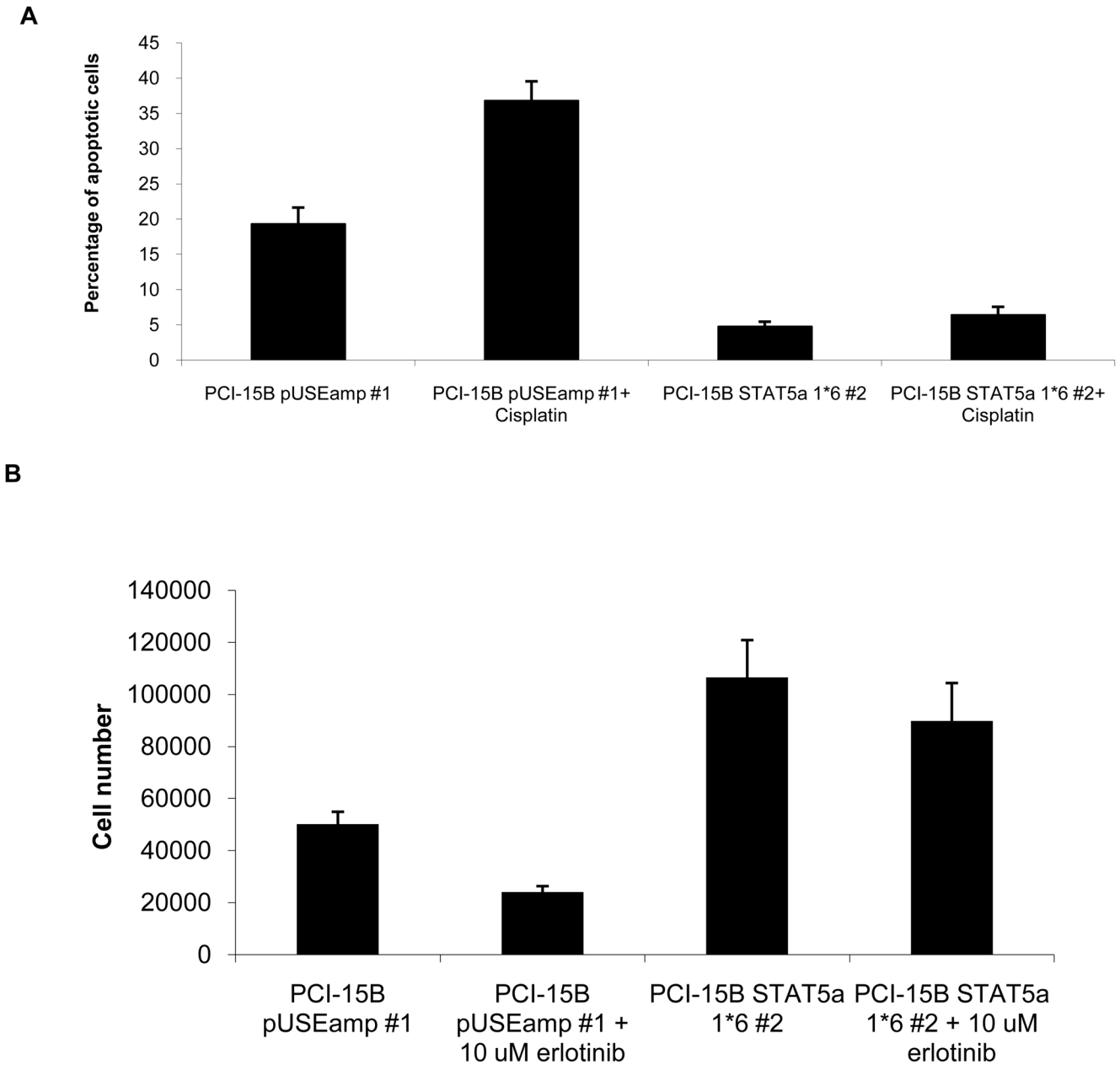

Figure 6. Activation of STAT5 increases resistance to cisplatin-induced apoptosis and erlotinib-induced growth inhibition

(A) 0.4×10^5 cells of PCI-15B pUSEamp #1 and PCI-15B STAT5a 1*6 #2 were plated in complete DMEM, with or without 10 μM cisplatin. 24 hrs post drug treatment, cells were harvested for Annexin staining. 8–10 fields were quantified per sample in each experiment. The graph represents cumulative data from four independent experiments showing decreased apoptosis in response to cisplatin in the cells expressing dominant-active STAT5 ($p=0.0143$). (B) 0.2×10^5 cells each of PCI-15B pUSEamp #1 and PCI-15B STAT5a 1*6 #2 were plated in complete medium in 12-well plates. Twenty-four hours later, cells were treated with erlotinib (10 μM). Cell counts were performed 48 hours after treatment, using trypan blue vital dye exclusion. Percent inhibition of cell growth induced by erlotinib was calculated compared with DMSO treated controls for both PCI-15B pUSE amp#1 and

PCI-15B STAT5a 1*6 #2. The graph represents cumulative data from six independent experiments (p=0.0011).